P1.77 VARIANCE SCALING IN WATER VAPOR MEASUREMENTS FROM A TALL TOWER

KYLE G. PRESSEL * AND WILLIAM D. COLLINS

Department of Earth & Planetary Science, The University of California, Berkeley

ANKUR R. DESAI

Department of Atmospheric & Oceanic Sciences, The University of Wisconsin, Madison

1. Introduction

Numerous methods for the representation of subgrid-scale cloud variability in global climate models (GCMs) have been proposed and implemented. However, in general, these models lack a robust empirical foundation. In particular, statistical cloud models, which are based on an assumption that probability distributions of atmospheric moisture can be used as a basis for modeling subgrid-scale cloud variability have done little to advance beyond *ad hoc* specification of distributional form. Furthermore, statistical cloud models based upon distributional assumptions require specification of the statistical moments or equivalently, the parameters of the distribution which represent subgrid-scale moisture variability. Neither the statistical moments nor parameters have been explored empirically in detail. The primary obstacle to empirical justification of these methods is a lack of adequate global high vertical resolution profiles of atmospheric moisture at horizontal resolutions sufficient to resolve variability at length scales relevant to local cloud process.

Many studies have considered small scale moisture variability, but most are limited to a small set of meteorological conditions and locations. Thus, the available observations do not span the set of conditions within which a GCM cloud model is expected to perform. Several studies have used satellite measurements to assess the global distribution of moisture. However, these studies have lacked the vertical and horizontal resolution necessary to adequately address the statistical cloud modeling problem. The Atmospheric Infrared Sounder (AIRS) aboard NASA's Aqua satellite provides higher vertical and horizontal resolution than previous satellites. The horizontal resolution of AIRS continues to limit its ability to directly observe the subgrid-scale variability relevant to the statistical cloud modeling problem.

One possible means of approximating the statistical moments at length scales smaller than the directly measured scales is to use scaling properties of the moments. If the spectra of a particular moment $Q(l)$ for a particular field of data exhibits power law dependence on lenghtscale l then the field is said to exhibit scaling of that moment. For example, if a moment spectrum exhibits scaling across a range of scales bounded above by L_{min} and below by L_{max} then,

$$\forall l' \in (L_{min}, L_{max})$$
$$Q(l') = Cl^{\alpha}$$

where C is a constant and α is the scaling exponent. Thus,

$$\log\left(Q\left(l'\right)\right) = \log\left(C\right) + \alpha\log(l),$$

so that across the range of scales exhibiting scaling a spectrum will appear linear when plotted on log-log axes.

Kahn and Teixeira (2009) laid the ground work for using the scaling properties of AIRS water vapor measurements to extract information meaningful to the statistical cloud modeling problem. In particular, they have shown using poor man's variance scaling analysis that AIRS measurements of water vapor exhibit variance scaling across a wide range of length scales with no apparent scale breaks. Poor man's variance scaling analysis, as described by Lorenz (1979), computes the variance spectra of a spatially distributed data set by computing the mean variance of subsets of the data having a particular spatial extent for a range of subset sizes. Kahn and Teixeira (2009) argue that in light of previous studies (using aircraft based measurements) which have found similar scaling with no scale breaks, there may be justification for using scaling to extend statistics measured at larger scales to smaller scales.

* *Corresponding author address:* Kyle G. Pressel, The Department of Earth and Planetary Sciences The University of California, Berkeley, Berkeley, CA 94720.
E-mail: pressel@berkeley.edu

In this paper we describe a methodology for using high temporal resolution observations of water vapor mixing ratio from a very tall tower to investigate spatial scaling of water vapor variance at length scales in excess of the boundary layer height. Using a tower based observational platform allows for near continuous measurement across a wide variety of meteorological conditions. Additionally, we will describe the use of observations of carbon dioxide (CO_2) mixing ratio at multiple heights to classify observed tower time time series as being in or above the mixed layer. Finally, we will attempt to reconcile tower observed scaling exponents with previous studies and existing theory.

2. Data and Methods

The WLEF tower located near Park Falls, Wisconsin (45.94591N latitude, 90.27231W longitude) is a 447m tall television broadcast tower (Davis et al. 2003). The tower is outfitted with high precision gas analyzers and sonic aneomometer which provide 10Hz measurements of water vapor mixing rato, three dimensional wind velocity, and virtual sonic temperature at the 396, 122, and 33m levels. Water vapor mixing ratio is measured by transporting sampled air from tower levels through a 1/4" outer diameter tube to gas analyzers located at ground level (Berger et al. 2001). This measurement technique may lead to underestimation of variability at small scales. CO_2 mixing ratio is measured at the 11, 30, 76, 122, 244, and 396m levels using a high precision gas analyzer.

Exploring the spatial variability of water vapor using an *in situ* point measurement requires using Taylor's hypothesis to transform data series which are distributed in time to data series approximately distributed in space. Taylor's hypothesis supposes that if the energy contained in turbulence is small relative to the energy of the mean flow, then a data series observed at times t_i can be regarded as a data series observed at locations x_i where,

$$x_i \approx \bar{u} t_i$$

and $\bar{u}$ is the mean horizontal wind velocity. In this study, two hour time series are randomly subsampled from a daily time series of water vapor mixing ratio and horizontal wind velocity from the 396 and 122m WLEF tower levels. In order to span a broad set of large scale of meteorological conditions we analyze data collected during December 2006 and July 2007. Each two hour subsampled time series is quality controlled to ensure that the observational height is entirely cloud free and to ensure that the assumptions necessary to apply Taylor's hypothesis approximately hold. The subsampled time series are then de-trended by subtracting the best fitting second order polynomial from the series. Henceforth, each subsampled time series will be referred to as a time series.

For each quality controlled time series, poor man's standard deviation spectra are computed. These spectra are constructed by computing the mean standard deviation of randomly selected time intervals of a single interval length. The mean standard deviation for a particular time interval length corresponds to the value of the standard deviation spectra at a length scale equal to that interval size. The length scale for each time interval length is determined using Taylor's hypothesis with the two hour mean horizontal wind speed. The largest length scale for which the spectra are computed is equal to one half of the length of the total subset as determined by Taylor's Hypothesis.

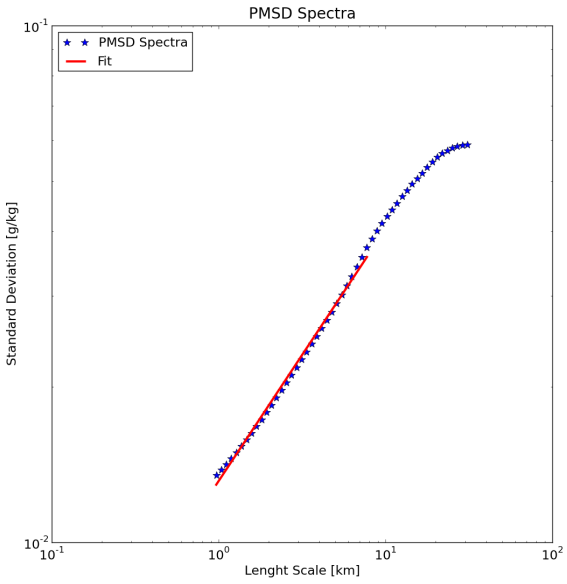

Figure 1: An example of a poor man's standard deviation spectrum computed from a single time series. The value of standard deviation for a particular wave length is indicated by a. The red line is the best fitting power-law to the spectra

Figure 1 shows a typical poor man's standard deviation spectrum computed from a single time series. In particular a gradual roll off to near constant values of standard deviation at large scales is characteris-

tic of many time series. The exact location of this roll-off often marks the largest scales at which scaling is observed. Because this study is interested in assessing the scaling of water vapor at large scales relative to the boundary layer depth it is important to precisely determine the largest scale at which scaling is observed. The gradual roll-off at large scales makes this difficult. We use the first order structure function of the water vapor series to determine the maximum length scale of observed scaling.

The first order structure function for a one dimensional discrete variable $\mathcal{Z}(x_i)$ is defined as

$$S^1_{\mathcal{Z}} =< |\mathcal{Z}(x_i + l) - \mathcal{Z}(x_i)| >$$

where l is the lag distance and $<>$ indicates the mean over all x_i such that $x_i + l \leq \max(x_i)$. In theory, $<>$ represents an ensemble average, however in practice the arithmetic mean is computed over all lag pairs. Figure 2 shows the first structure function computed for the same data used to compute the poor man's standard deviation spectrum shown in Figure 1. Because the first structure function and poor man's standard deviation spectra contain very similar information about the spatial variability of the field, both exhibit scaling (a linear region in Figures 1 and 2) across a similar range of length scales. However, in this particular instance, and in many others, the break from uniform scaling of the structure function appears not as a gentle roll-off but as a sharp angle near its maximum value. The leveling off of the structure function to a near constant value is related to the transition from non-stationary to stationary scaling associated with the spatial integral scale (Marshak et al. 1997). This suggests that the maximum value of the first structure function can be used to more precisely determine the maximum length scale at which it is appropriate to determine scaling exponents from a poor man's spectra.

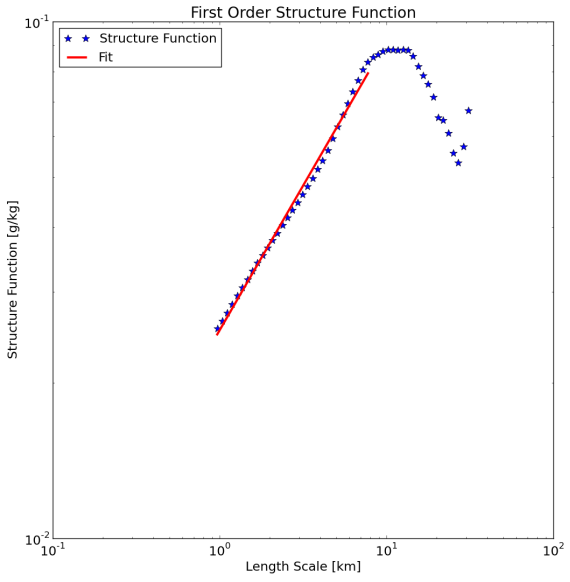

Figure 2: An example of the first structure function computed for the same data as the poor man's standard deviation spectrum shown in Figure 1.

Upon use of the first structure function to determine an approximate maximum scaling length scale, scaling exponents are computed by least squares fit to the poor man's standard deviation spectra between 1.05 km and the approximate maximum scaling length scale, which we specify as the length scale of the first point in the structure function to exceed 95% of the structure function's maximum value. In order to assess the degree to which a power law can be used to model the spectra, the correlation coefficient between the log poor man's spectrum and linear least squares fit to the log poor man's spectrum is computed. We consider a particular poor man's spectra to exhibit scaling if the correlation coefficient of the linear fit at scales up to the maximum scaling length scale is greater than 0.90. The algorithm exhibits some sensitivity to the selection of the minimum correlation coefficient, a full characterization of this sensitivity is the subject of ongoing and future work.

Ideally, a single spectrum and structure function would be computed for a large ensemble of time series observed under identical meteorological conditions. In practice this is extremely difficult. Therefore, time series and associated poor man's scaling exponents are composited into classes having similar meteorological conditions. The two most obvious and general composite classes are for time series observed within or not within the mixed layer.

In order to determine if a particular time series is contained entirely within the convective mixed-layer we use a modified version of an algorithm described by Yi et al. (2001), which uses the tower observed vertical gradients of CO_2 to determine the top of the convective mixed layer. The basic premise of the algorithm is that the large nocturnal biogenic flux of CO_2 into the atmosphere leads to a large vertical gradient of CO_2 across the top of the boundary layer, while within the boundary layer mixing leads to a weaker CO_2 gradient. During the daytime there is likely a significant flux of CO_2 out of the boundary layer by photosynthetic activity which may reduce vertical gradients, however we assume that

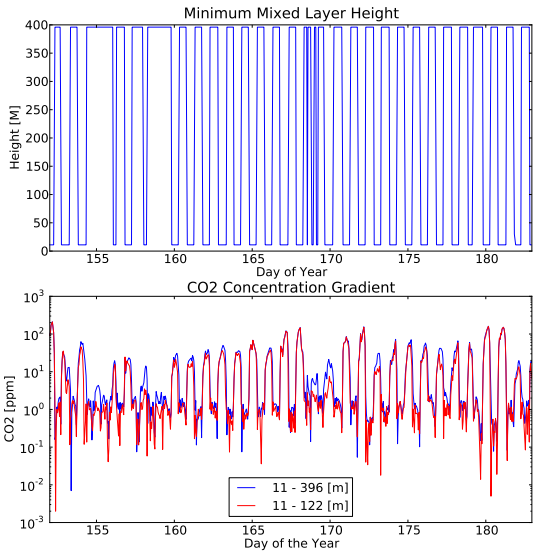

Figure 3: (**Top Panel**) The minimum mixed layer height as determined determined from CO_2 gradient. (**Lower Panel**) The difference between CO_2 concentrations between 396 and 11m in blue and 122 and 11m in red.

strong convectively driven turbulent mixing will play the dominant role in dissipating gradients of CO_2. In particular, our algorithm assumes that if the difference in measured CO_2 mixing ratio between the observational level and the surface (11m level) is below a threshold value then the observational level is contained within the mixed-layer.

The top panel of Figure 3 shows the minimum mixed-layer height as determined from the CO_2 concentration differences shown in the lower panel. Notice that the diurnal range in CO_2 difference is often in excess of two orders of magnitude. We define the minimum mixed-layer height as the highest tower level which is contained within the mixed-layer.

The CO_2 based mixed layer identification algorithm is applied to each time series to determine if an entire time series was observed from within a mixed layer. If a time series spans a transition from mixed layer to non-mixed layer conditions it is not included in the analysis.

We present histograms of the scaling exponents for each case in order to identify commonly occurring ranges of scaling exponents. As a preliminary step towards understanding the scaling exponents which characterize the scale dependence of variance in the lower atmosphere, we compute kernel density estimates of the mixed layer and non-mixed layer scaling exponents for the 122m and tower level during the month of December 2006 and the 122m and 396m tower levels during June 2007. We use the maximum of the kernel density estimates to approximate the location of the dominant mode in scaling exponent histograms.

3. Results

The spatial scaling properties of many geophysical variables have been investigated empirically and theoretically, and interpretation of our results is best done in the context of these previous studies. In particular, the similarity hypothesis proposed by Kolmogorov (1941) suggested the existence of a scaling law of the form

$$S_v^1(l) \sim l^{\frac{1}{3}} \tag{1}$$

for the three dimensional first order structure function of velocity in fully developed turbulent flow. The Wiener-Khinchin Theorem allows scaling exponents of the first structure function to be related to Fourier power spectra exponents through the equation

$$\beta = -(2\alpha_{struct} + 1) \tag{2}$$

where β and α_{struct} are respectively the power spectra and structure function scaling exponents. Note that using equation 2 to convert the scaling exponent from equation 1 into a Fourier power spectra exponent gives β = -5/3, which is the well known energy cascade for fully developed turbulence. Kahn and Teixeira (2009) point out that an analog to equation 2 for the relationship between Fourier power spectra exponents and poorman's scaling exponents is not expected to hold explicitly, but due to the similarity between poorman's spectra and structure functions it may hold in an approximate sense. To allow comparison of our results to those of others we assume,

$$\beta \approx -(2\alpha + 1) \tag{3}$$

where α is the poor man's standard deviation spectra scaling exponent.

Charney (1971) used scaling analysis to predict the existence of an $\alpha_{struct} = 1$ scaling for velocity and temperature variance associated within a region of the spectra characterized by a quasi-equlibrium cascade of enstrophy from large to small scales. Gage and Nastrom (1986) used observations of temperature and winds from commercial aircraft to investigate scaling across scale ranging from 3km to 3000km at elevations between 9km and 14km. In

particular they found that at large scales both temperature and wind velocity spectra were characterized by α_{struct} = 1 spectra large scales ($>$ 700 km) and α_{struct} = 1/3 at smaller scales. Using the same dataset Nastrom et al. (1986) showed that water vapor exhibited α_{struct} = 1/3 scaling between 150km and 3000km. Tjemkes and Visser (1994) observed α_{struct} = 1/3 scaling in satellite observations of water vapor at scales down to 50km at multiple pressure levels.

We now turn to our analysis of scaling in tower observed time series of water vapor mixing ratio using poor man's scaling analysis.

a. *June 2007*

Table 1 gives the percentage of sample time series which exhibit scaling to scales in excess of 5km and the scaling exponent of the kernel density estimate maximum for each of the four cases considered during June 2007. For all cases the majority of all time series exhibit scaling to scales in excess of 5km, suggesting scaling poor of man's variance spectra is a robust feature of the lower troposphere. Figures 4, 5, 6, 7 are histograms of the scaling exponents for the 396m non-mixed layer, 396m mixed layer, 122m non-mixed layer, and 122m mixed layer cases respectively. The histograms of scaling exponents are generally unimodal with the exception of the 396m mixed-layer case where there is a second mode near 1/2 (0.5).

The peaks of all histograms are between 1/4 (0.25) and 2/5 (0.4), however the peaks evident in the histograms and scaling exponent of the maximum of the kernel density estimate of the 122m non-mixed layer and 396m mixed layer cases are close to the $1/3$ (0.33) value expected from Kolmogorov's similarity argument for fully developed turbulence as well those reported in previous observational studies.

	122m	396m
Non-Mixed Layer	81.0% ; 0.34	80.4% ; 0.39
Mixed Layer	68.3% ; 0.25	70.8% ; 0.35

Table 1: Scaling exponent of kernel density estimate maximum and percentage of sampled time series which exhibit scaling in excess of 5km for June 2007.

b. *December 2006*

Table 1 gives the percentage of sampled time series which exhibit scaling to scales in excess of 5km

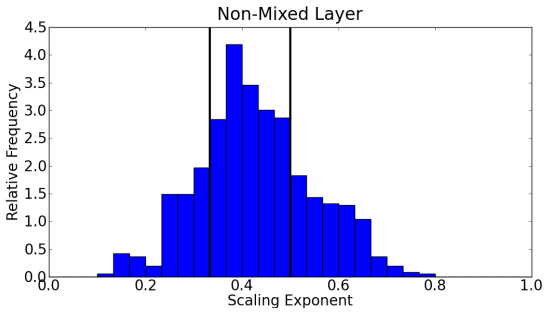

Figure 4: June 396m Non-Mixed Layer Histogram

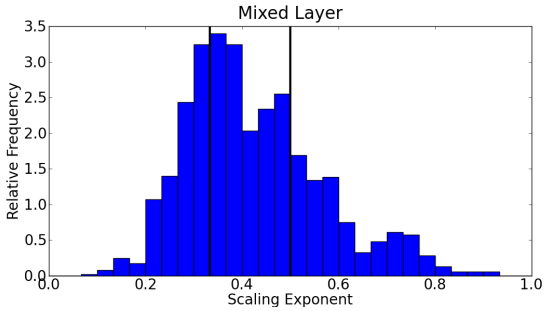

Figure 5: June 396m Mixed Layer Histogram

and the maximum of the scaling exponent kernel estimate for each of the two cases considered during December 2007. Figures 9 and 8 are respectively, the histograms of scaling exponents for the mixed layer and non-mixed layer cases. The histograms for both mixed and non-mixed layer cases are strongly bimodal with the dominant mode being near 0.3 in both cases. A second less dominant mode occurs near above 0.5 in both histograms. We have decided to omit results from 122m level for December 2006 observations because of some question as to the integrity of these observations. Verification of the integrity of this data is the subject of future work.

	396m
Non-Mixed Layer	90.3% ; 0.26
Mixed Layer	95.2% ; 0.33

Table 2: Scaling exponent of kernel density estimate maximum and percentage of sampled time series which exhibit scaling in excess of 5km for December 2007.

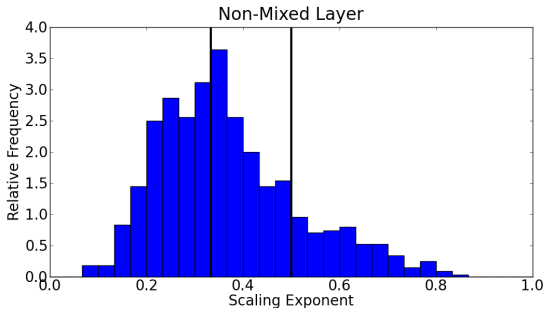

Figure 6: June 122m Non-Mixed Layer Histogram

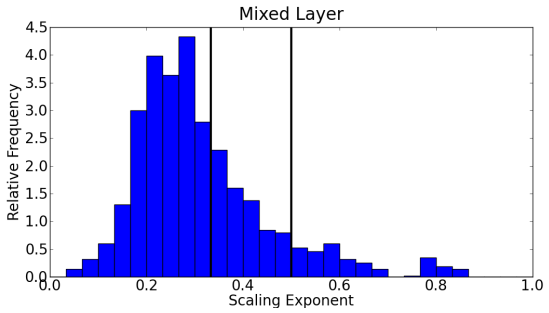

Figure 7: June 122m Mixed Layer Histogram

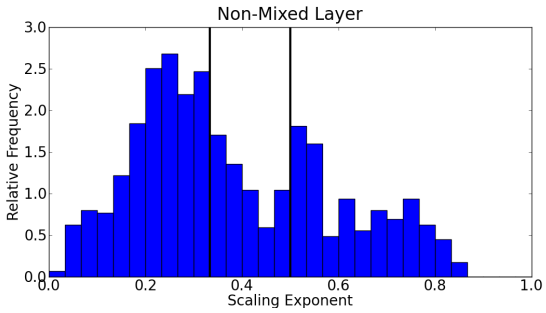

Figure 8: December 396m Non-Mixed Layer Histogram

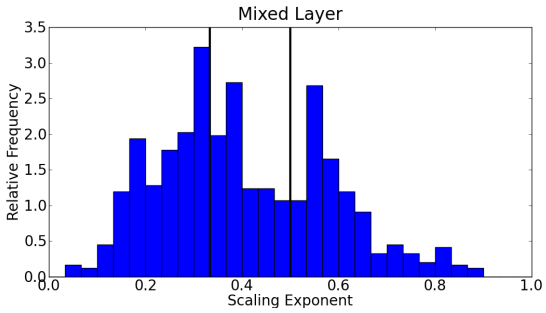

Figure 9: December 396m Mixed Layer Histogram

4. Analysis and Conclusions

Scaling of poor man's standard deviation spectra to scales in excess of 5km appears to be a robust feature of the lower troposphere. There is good agreement across all cases that scaling exponents in a range from $1/5$ (0.20) to $2/5$ (0.40) frequently characterize this scaling. The dominant peak in scaling exponent histograms for the June 122m non-mixed layer, June 396m mixed layer, and December 396m mixed layer occur very near $1/3$ (0.33) which stands in agreement with Kolmogorov's similarity and observational studies. For all cases the maximum in kernel density estimate is contained within the interval 0.33 ± 0.06. Given that we have not fully characterized the error associated with the method of analysis used in this study, it is difficult to make any strong statement regarding the differences between cases being significant. However, the apparent dominance of a small range of scaling exponents across a large range of meteorological conditions may suggest some degree of universality in scaling in which scaling exponents appear somewhat independent of large scale meteorological conditions.

The processes responsible for generating the secondary modes in the June 396m mixed layer, December 396m mixed, and December 396m non-mixed layer histograms are somewhat uncertain. However, the larger scaling exponents indicate that variance increases more rapidly with length scale, and it may prove fruitful to investigate the water vapor time series characterized by these larger exponents in more detail.

Of particular interest is that scaling of water vapor variance appears to frequently exist at scales in excess of the boundary layer height. This is interesting because the height of the boundary layer imposes a maximum vertical length scale on eddies within the boundary layer. Thus, it is somewhat surprising to see that the spatial integral scale is so often much larger than the boundary layer height which would typically be expected to be less than 2km.

Characterizing the errors associated with this analysis method is the subject of ongoing research. In particular we seek to assess the errors associated with the approximation given in equation 3. The accuracy of this approximation determines the degree to which poor man's scaling exponents can be compared to results using Fourier and structure function analysis.

These results coupled with the results of Kahn

and Teixeira (2009), and citations of previous studies therein, continue to lend support for the use of water vapor variance scaling to estimate the variance at scales smaller than satellite observed scales. The true promise of utilizing the scaling properties of the water vapor field to extend observations at large scales to the smaller scales relevant to the parameterization of clouds and radiation in global climate models is the union of theory and empiricism it affords. Furthermore, a tremendous body of literature exists in other disciplines which take advantage of the universality of scaling processes in turbulent fluids to construct parameterizations of sub-gridscale phenomena. Confirming a similar universality for water vapor scaling at resolutions near global climate model gridscale holds particular promise for the improvement of the parameterization of moist processes in these models.

5. Acknowledgement

We acknowledge the NASA Interdisciplinary Science Program and support of WLEF tower observations from NOAA Earth System Research Lab, Department of Energy (DOE) National Institute for Climatic Change Research (NICCR) Midwestern Region Subagreement 050516Z19, and the National Science Foundation (NSF) Biology Directorate Grant DEB-0845166.

WLEF flux tower measurements were made possible via tireless efforts of K.J. Davis of Penn State University, J. Thom of University of Wisconsin-Madison, B.D. Cook of NASA Goddard Space Flight Center, R. Teclaw and D. Baumann of the U.S. Forest Service Northern Research Station, and R. Strand, of the Wisconsin Education Communications Board (ECB).

References

Berger, B. W., K. J. Davis, C. Yi, P. S. Bakwin, and C. L. Zhao, 2001: Long-term carbon dioxide fluxes from a very tall tower in a northern forest: Flux measurement methodology. *Journal of Atmospheric and Oceanic Technology*, **18**, 529–542.

Charney, J., 1971: Geostrophic Turbulence. *Journal of Atmospheric Sciences*, **28**, 1087–1094.

Davis, K., P. Bakwin, C. Yi, B. Berger, C. Zhao, R. Teclaw, and J. Isebrands, 2003: The annual cycles of CO2 and H2O exchange over a northern mixed forest as observed from a very tall tower. *Global Change Biology*, **9**, 1278–1293.

Gage, K. and G. Nastrom, 1986: Theoretical interpretation of atmospheric wavenumber spectra of wind and temperature observed by commercial aircraft during GASP. *Journal of the Atmospheric Sciences*, **43**, 729–740.

Kahn, B. and J. Teixeira, 2009: A global climatology of temperature and water vapor variance scaling from the Atmospheric Infrared Sounder. *Journal of Climate*, **22**, 5558–5576.

Kimmel, S. J., J. C. Wyngaard, and M. J. Otte, 2002: Log-chipper turbulence in the convective boundary layer. *Journal of the Atmospheric Sciences*, **59**, 1124–1134.

Kolmogorov, A., 1941: On degeneration of isotropic turbulence in an incompressible viscous liquid. *Comptes Rendus (Doklady) de lAcademie des Sciences de lU.R.S.S.,*, **31**, 538–540.

Lorenz, E., 1979: Forced and free variations of weather and climate. *Journal of the Atmospheric Sciences*, **36**, 1367–1376.

Marshak, A., A. Davis, W. Wiscombe, and R. Cahalan, 1997: Scale invariance in liquid water distributions in marine stratocumulus. part ii: Multifractal properties and intermittency issues. *Journal of the Atmospheric Sciences*, **54**, 1423–1444.

Nastrom, G., W. Jasperson, and K. Gage, 1986: Horizontal spectra of atmospheric tracers measured during the Global Atmospheric Sampling Program. *Journal of Geophysical Research*, **91**, 13201–13209.

Tjemkes, S. and M. Visser, 1994: Horizontal variability of temperature, specific humidity, and cloud liquid water as derived from spaceborne observations. *Journal of Geophysical Research*, **99**, 23089–23105.

Yi, C., K. Davis, B. Berger, and P. Bakwin, 2001: Long-term observations of the dynamics of the continental planetary boundary layer. *Journal of the Atmospheric Sciences*, **58**, 1288–1299.